Supporting Information

Arabidopsis YAF9 histone readers modulate flowering time through NuA4-complex-dependent H4 and H2A.Z histone acetylation at *FLC* chromatin

Authors: Pedro Crevillén, Ángeles Gómez-Zambrano, Juan A. López, Jesús Vázquez, Manuel Piñeiro and José A. Jarillo

Fig. S14 YAF9A protein directly binds *FT* chromatin and mediates in the deposition of H2A.Z in this locus.

Fig.S15 Characterization of the Arabidopsis YAF9A-TAPa 3 and 10 lines generated.

Table S1 List of primers used in this study.

Table S2 List of cell cycle-related genes misregulated in *yaf9yaf9b*.

Table S3 List of SAR-related genes deregulated in *yaf9yaf9b*.

Datasets:

Dataset S1 List of differentially expressed genes in *yaf9a yaf9b*.

Dataset S2 Arabidopsis YAF9A protein interactors.

Methods S1 Supporting information and Methods.

Fig. S1 Two Arabidopsis YEATS domain-containing proteins are the predicted homologs of yeast YAF9 protein. (a) Neighbour-joining protein sequence phylogeny showing all the *Arabidopsis thaliana* (YAF9A and YAF9B), *Saccharomyces cerevisiae (*Yaf9, Sas5 and Taf14) and *Schizosaccharomyces pombe* (Yaf9 and Tfg3) YEATS domain containing proteins. The analysis was performed on the Phylogeny.fr web platform and comprised the following steps: first sequences were aligned with MUSCLE, after alignment, ambiguous regions were removed with Gblocks; last, the phylogenetic tree was reconstructed using the maximum likelihood method. (b) Sequence comparisons of YAF9 proteins from different organisms using ClustalX v1.81: At, *Arabidopsis thaliana*; Os, *Oryza sativa*; Dm, *Drosophila melanogaster*; Ce, *Caenorhabditis elegans*; Sc, *Saccharomyces cerevisiae*. Blue line box indicates the YEATS domain (IPR005033), and the red and green boxes refer to the A and B coiled coil boxes, respectively (Zhang *et al.*, 2004), which are conserved in YAF9 proteins.

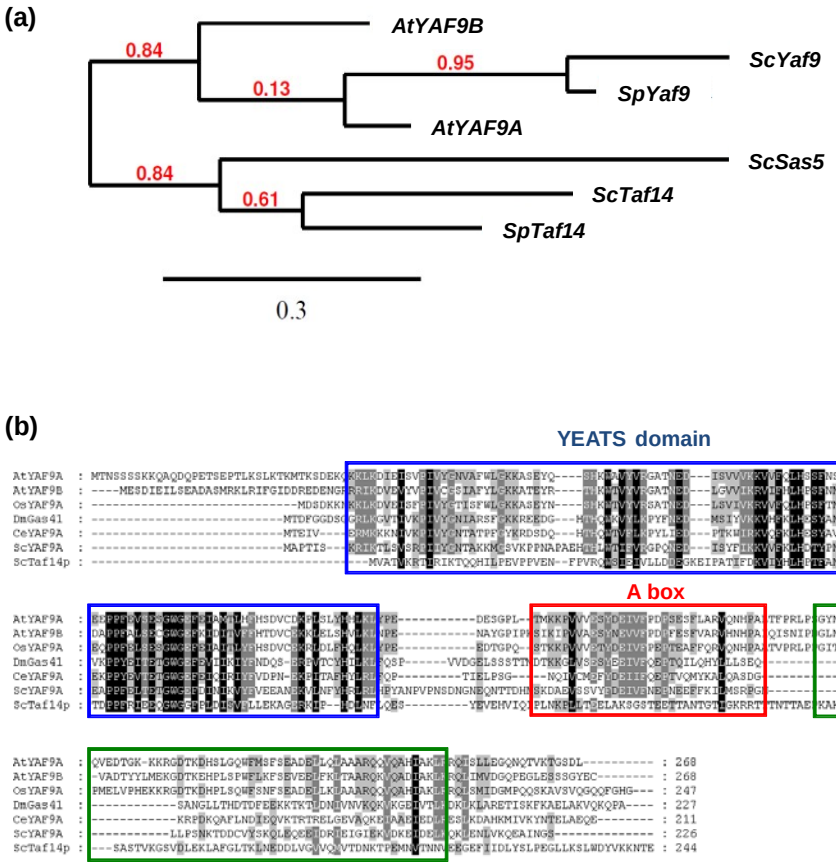

Fig. S2 The two Arabidopsis YAF9 proteins are nuclear localized but differentially expressed. (a) *YAF9A* and *YAF9B* expression pattern in different organs determined by quantitative RT-PCR and normalized against *UBQ10* expression (S, seedling; R, Roots; RL, rosette leaves; MS, main stem; CL cauline leaves; FB, flower buds; F, flowers). (b-c) *Agrobacterium*-mediated transient expression of the *35S::AtYAF9A-GFP* (b) and *35S::AtYAF9B-GFP* (c) constructs in nuclei of epidermal cells in *N. benthamiana* leaves. Images were taken with 20x (b) and 40x (c) magnification objectives. Small red arrows mark fluorescent nuclei.

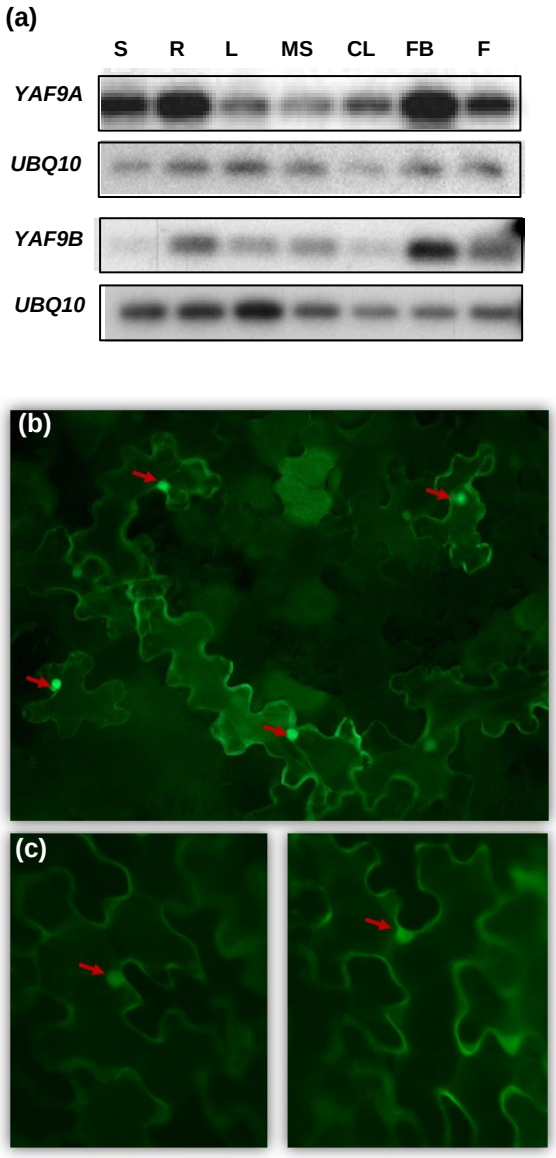

Fig. S3 Isolation of Arabidopsis *YAF9* knock-out mutants. (a-b) Schematic representation of *yaf9a-1* (a) and *yaf9b-2* (b) T-DNA insertional alleles. (c-e) *yaf9a-1* and *yaf9b-2* are knock-out mutants. Quantitative RT-PCR (c-d) and real time Q-PCR (e) assays for checking the expression of *YAF9A* and *YAF9B* in seedlings of single and double *yaf9* mutant combinations. Error bars indicate ± standard error of the mean (s.e.m) (n=3).

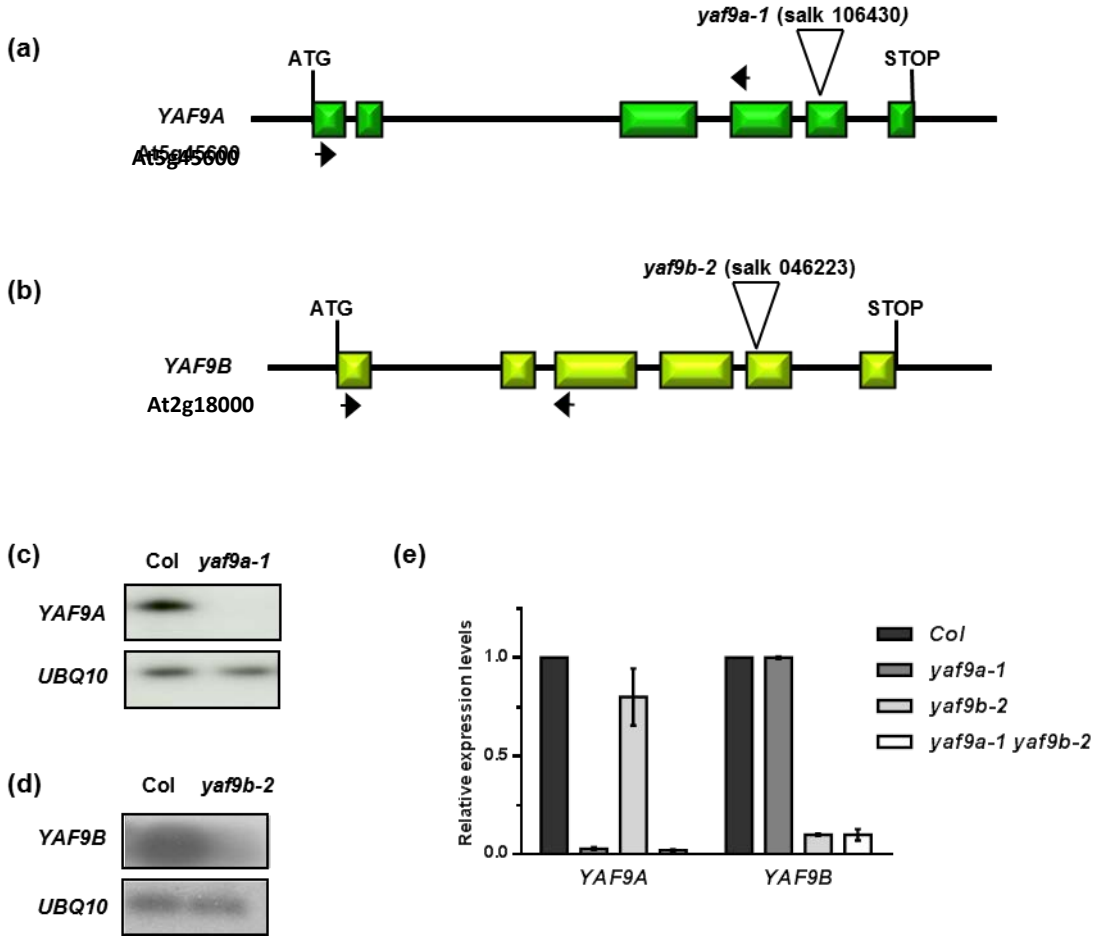

Fig. S4 Double mutant *yaf9a yaf9b* plants display a broad range of pleiotropic developmental defects. (a-b) Pictures of Col, *yaf9a*, *yaf9b* and *yaf9a yaf9b* mature plants grown under LD photoperiods (a) and 15-day old seedlings grown vertically on plates (b). (c-d) *yaf9a yaf9b* double mutant seedlings show reduced chlorophyll content (error bars indicate ± standard deviation n=3) (c) and shorter roots (error bars indicate ± standard deviation n=7) (d), compared to Col.

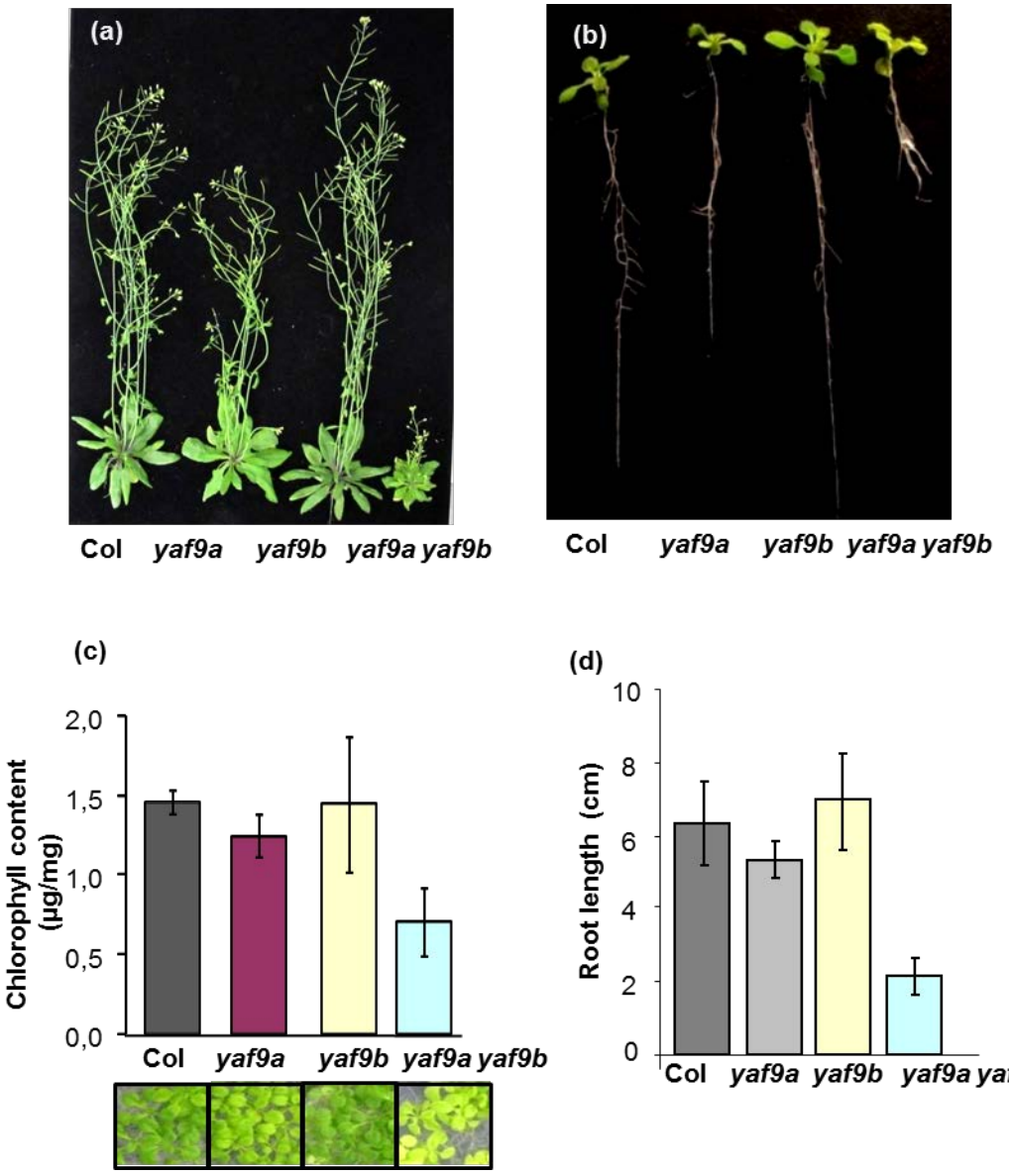

Fig. S5 Complementation of the *yaf9a* mutant with a wild type copy of the *YAF9A* gene. (a-b) The early flowering phenotype of the *yaf9a* mutant is complemented by a *35S::Myc-YAF9A* gene construct. Flowering time (a) of Col, *yaf9a, yaf9b* and *yaf9a yaf9b* mutants plus the transgenic *yaf9a 35S::Myc-YAF9A* line grown in LD. Error bars indicate s.e.m (n=16). (b) Q-PCR analysis showing the *YAF9A* expression levels in *yaf9a 35S::Myc-YAF9A* seedlings. Error bars indicate standard deviation (n=2).

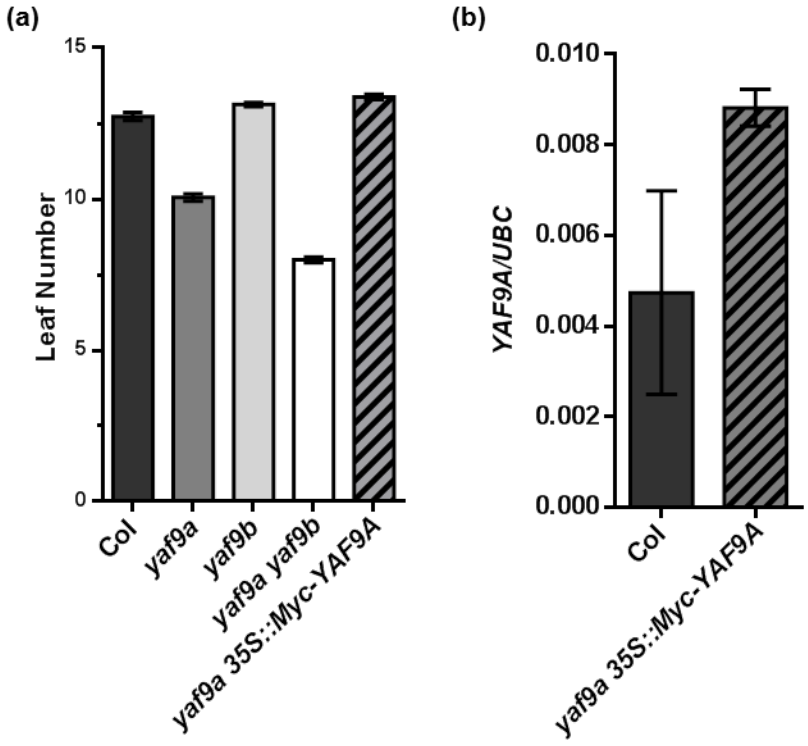

Fig. S6 Validation of microarray data obtained in the transcriptomic analysis of *yaf9ayaf9b* seedlings. Q-PRC expression analysis of selected misregulated genes from *yaf9a yaf9b* microarray data (Dataset S2). Relative gene expression was normalized to *ACT2* gene. Data represent the average of three biological replicates; error bars indicate ± standard deviation Primers used are described in Table S1.

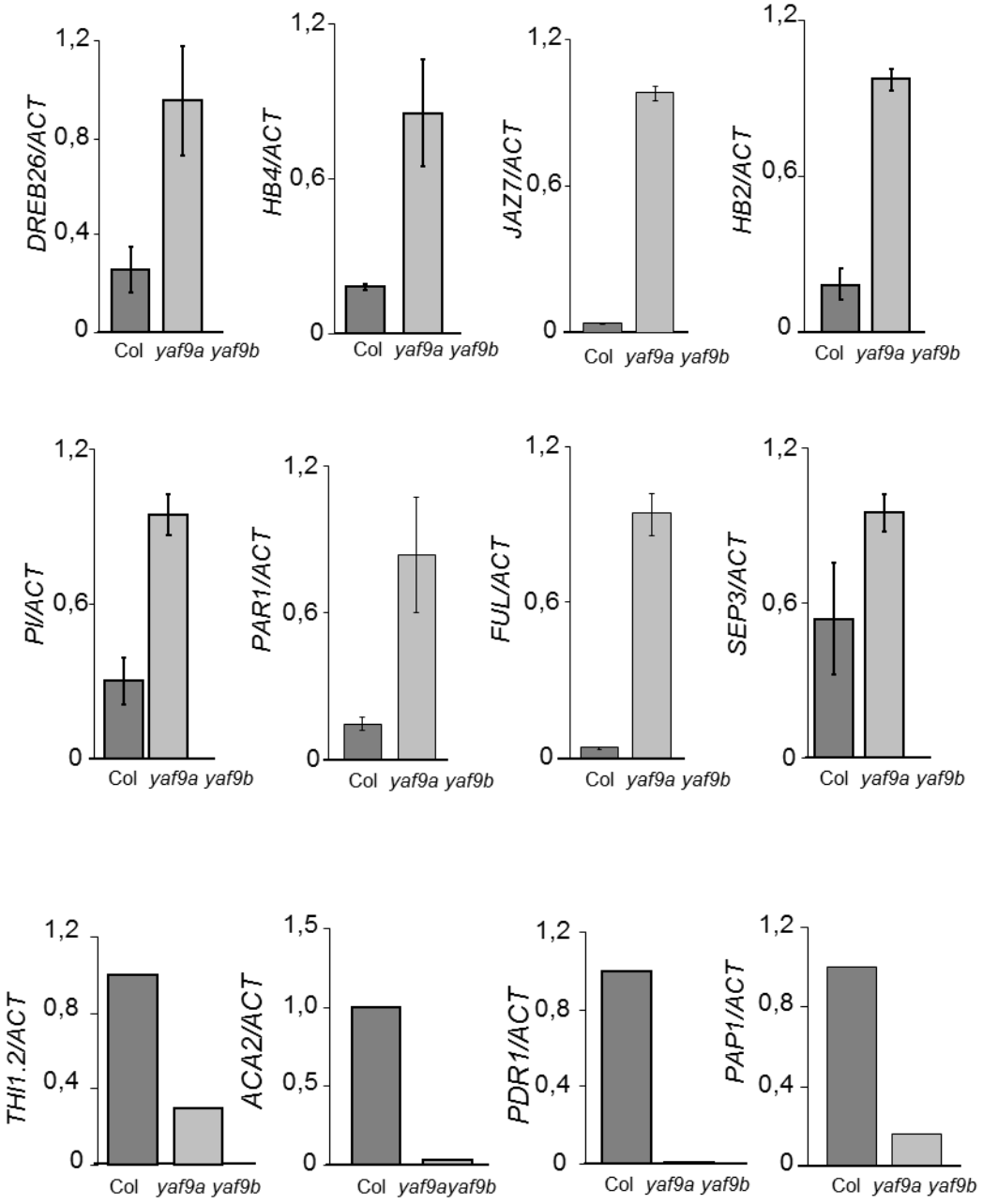

Fig. S7 Comparison of upregulated genes in *yaf9a yaf9b* seedlings and in selected *swr1-c* mutants. (a) Venn diagrams showing the overlap of upregulated genes between *yaf9a yaf9b* and other representative *swr1-c* mutants or plants depleted in H2A.Z. RNA seq analysis and published transcriptomic data ($log_2FC \geq 0.5$) from *arp6-10* (Kumar and Wigge, 2010), *pie1-5* (March-Diaz et al., 2008), *swc4i* (Gomez-Zambrano et al., 2018), *hta8,9,11* triple mutant (Coleman-Derr and Zilberman, 2012) and *swc6-1*, *arp6-1*, *pie1-2* and *hta9 hta11* mutants (Berriri et al., 2016) were used in the comparisons.(b) Statistical significance of the overlap of the upregulated genes in the *swr1-c* mutants with *yaf9a yaf9b* upregulated genes was determined performing a hypergeometric test (***p≤0.001).

(a)

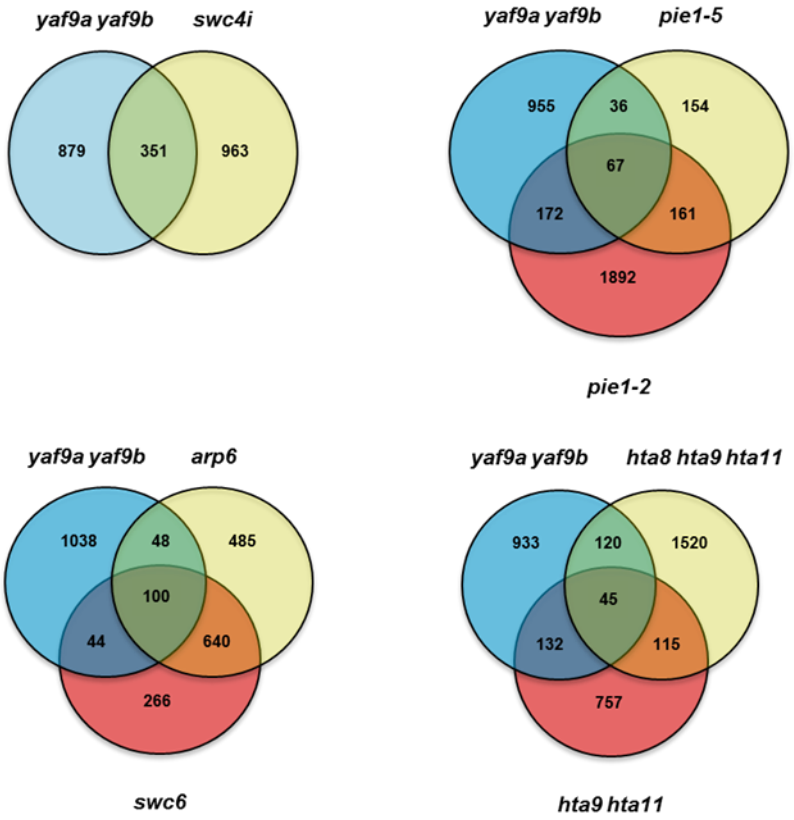

(b)

yaf9a yaf9b vs	p-value	score
swc4i	2.1E-26	***
swc6-1	3.3E-19	***
arp6-1	3.1E-19	***
pie1-2	1.8E-33	***
pie1-5	1.6E-38	***
hta9 hta11	9.9E-26	***
hta8 hta9 hta11	5.2E-11	***

Fig. S8 Comparison of downregulated genes in *yaf9a yaf9b* seedlings and in selected *swr1-c* mutants. (a) Venn diagrams showing the overlap of downregulated genes between *yaf9a yaf9b* and other representative *swr1-c* mutants or plants depleted in H2A.Z. RNA seq analysis and published transcriptomic data ($log_2FC \geq 0.5$) from *arp6-10* (Kumar and Wigge, 2010), *pie1-5* (March-Diaz et al., 2008), *swc4i* (Gomez-Zambrano et al., 2018), *hta8 hta9 hta11* triple mutant (Coleman-Derr and Zilberman, 2012) and *swc6-1*, *arp6-1*, *pie1-2* and *hta9 hta11* mutants (Berriri et al., 2016) were used in the comparisons.(b) Statistical significance of the overlap of the upregulated genes in the *swr1-c* mutants with *yaf9a yaf9b* upregulated genes was determined performing a hypergeometric test (ns, not significant; ***p≤0.001).

(a)

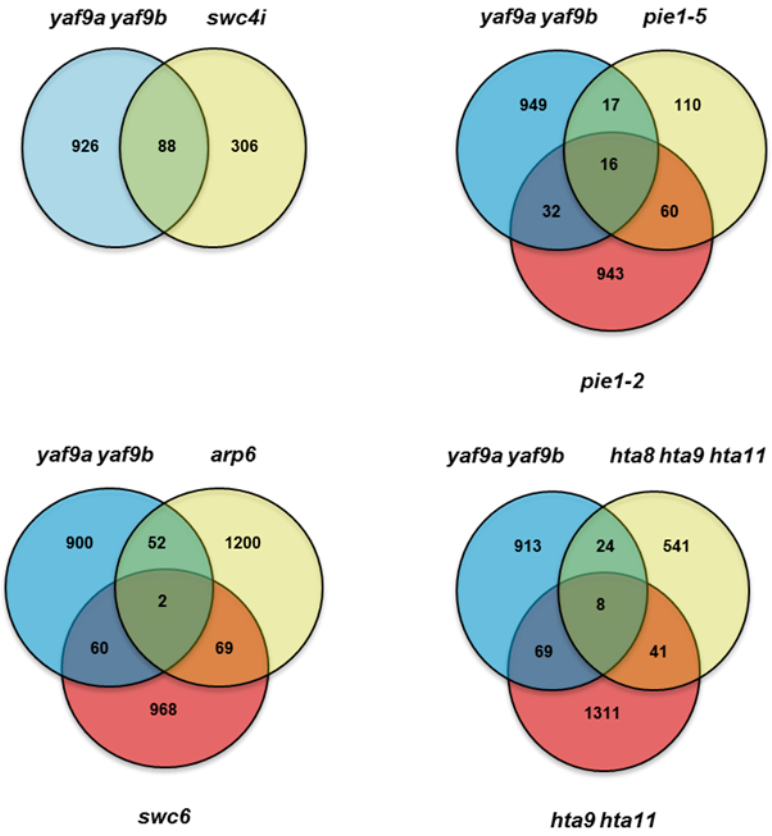

(b)

yaf9a yaf9b vs	p-value	score
swc4i	9.1E-34	***
swc6-1	1.8E-06	***
arp6-1	0.0127	ns
pie1-2	0.0068	ns
pie1-5	9.9E-15	***
hta9 hta11	3.4E-06	ns
hta8 hta9 hta11	0,00403	***

Fig. S9 Genome-wide transcriptomic analysis of *yaf9a yaf9b* mutant. (a) List of significant Biological Processes (GO terms) ranked from lowest (orange) to highest (blue) *p-value* (SEA AgriGO) derived from genes misregulated in *yaf9a yaf9b*. (b) List of genes related to flowering time regulation and flower development (GO:0009910; GO:0009909; GO:0009911 GO:0048573; GO:0048574; GO:0048833) ranked from highest (red) to lowest (blue) fold-change expression value.

(a)

GO term	*p-value*
response to stimulus	1,2E-38
response to stress	4,1E-26
response to endogenous stimulus	2,8E-14
response to abiotic stimulus	6,2E-12
response to biotic stimulus	3,2E-11
multi-organism process	1,3E-09
secondary metabolic process	1,1E-06
response to external stimulus	8,1E-06
metabolic process	1,3E-05
carbohydrate metabolic process	3,3E-05
biological regulation	5,3E-05
response to extracellular stimulus	2,0E-04
post-embryonic development	2,3E-04
cell growth	2,8E-04
regulation of biological quality	3,7E-04
regulation of cell size	4,8E-04
cellular process	5,3E-04
regulation of structure size	5,7E-04
regulation of cellular size	5,7E-04
lipid metabolic process	8,6E-04
growth	1,1E-03
localization	3,0E-03
biosynthetic process	3,1E-03

(b)

Transcript ID	Gene	FC
AT4G17460	*HAT1*	3,38
AT5G60910	*FUL*	3,37
AT5G37770	*TCH2*	2,69
AT2G33810	*SPL3*	2,25
AT1G24260	*SEP3*	2,01
AT2G38810	*HTA8*	2,00
AT4G24540	*AGL24*	1,60
AT5G08370	*AGAL2*	1,53
AT1G13260	*RAV1*	1,50
AT1G45050	*UBC15*	1,49
AT1G12610	*DDF1*	1,48
AT4G31120	*SKB1*	1,43
AT1G65480	*FT*	1,42
AT5G15840	*CO*	1,42
AT4G28190	*ULT1*	1,41
AT1G69490	*NAP*	-1,44
AT2G44680	*CKB4*	-1,45
AT1G65380	*CLV2*	-1,48
AT1G68050	*FKF1*	-1,56
AT5G15850	*COL1*	-1,58
AT1G26260	*CIB5*	-1,59
AT5G44190	*GLK2*	-1,68
AT2G20570	*GPRI1*	-1,90
AT5G10140	*FLC*	-1,95

Fig. S10 Singular Enrichment Analysis (SEA) of Gene Ontology (GO) terms of genes with altered expression in *yaf9a yaf9b* seedlings. Tree graph representation of over-represented GO terms in "biological process" category obtained using AgriGO (Fisher test statistical analysis, $p<0.05$). Significant terms are marked with colour; non-significant ones are shown in white boxes. This hierarchical graph is represented ranked from top to bottom.

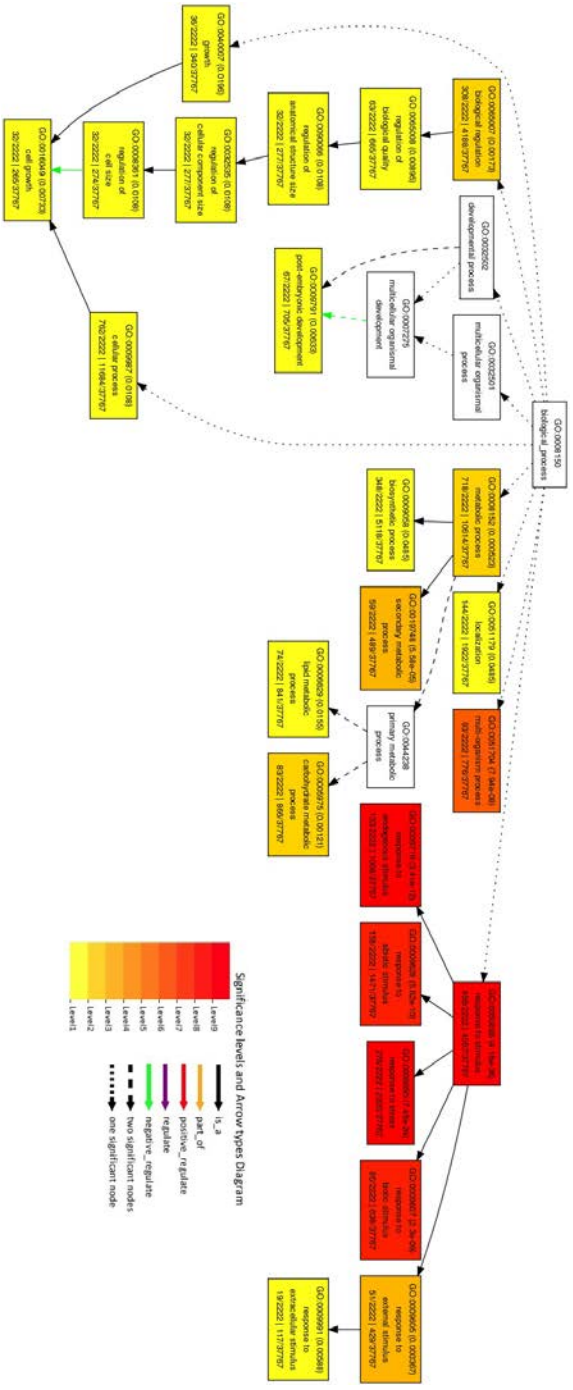

Fig. S11 *yaf9 ayaf9b* plants display necrotic spots and paler colour in the leaves than Col. Pictures were taken at 30 day-old plants grown in SD.

Col (WT)

yaf9a yaf9b

Fig. S12 Determination of the specificity of α-H2A.Zac antibody used in the ChIP analysis. (a-b) Histone protein extracts from Col seedlings, treated with and without sodium butyrate (NaBu), a potent inhibitor of deacetylases (a), or from Col and *hta9 hta11* seedlings treated with NaBu (b) were tested by western blot against α-H2A.Zac (Diagenode C15410173, Belgium) and α-H3 (Abcam ab1791,UK). H2A.Z acetylated signal is only detected in Col when seedlings are treated with NaBu (a) showing that the α-H2A.Zac antibody recognizes specifically acetylated histones. As shown in (b) we could not detect any H2A.Zac signal in histone extracts from *hta9 hta11* double mutant. The arrow in both panels indicates the expected size band for H2A.Zac. In most nuclear histone extract preparations, an extra band of smaller size was detected, possibly a proteolysis product or a truncated acetylated form of H2A.Z.

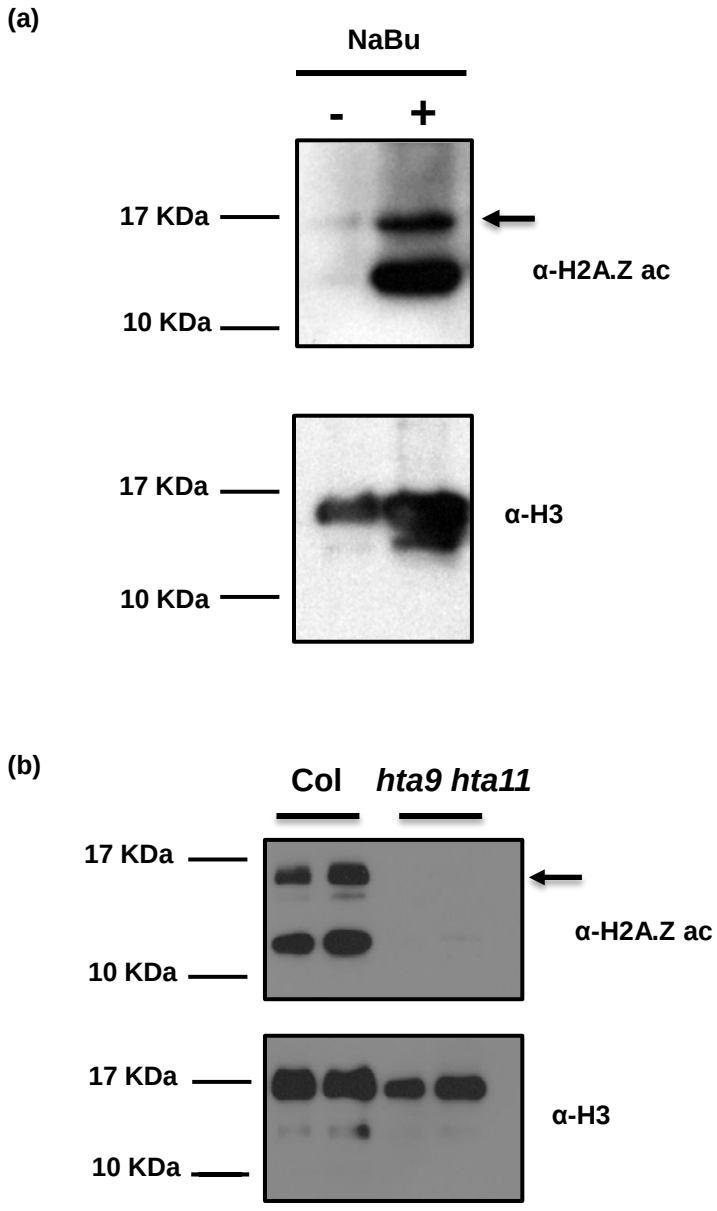

Fig. S13 *yaf9a* but not *yaf9b* mutants showed reduced histone H4 acetylation levels at *FLC* chromatin. (a) Schematic representation of *FLC* locus indicating the regions analyzed by ChIP. (b) ChIP experiments using α-H4ac in Col, *yaf9a, yaf9b* and *yaf9a yaf9b* mutant seedlings. Data are represented as the fraction of immunoprecipitated DNA normalized to an *ACT2* gene region. Graphs represent the average of two independent biological ChIP experiments quantified by Q-PCR. Error bars indicate standard deviation. Statistical significance was calculated using Student´s t-test. (n.s, not significant; *p≤0.05; **p≤0.01).

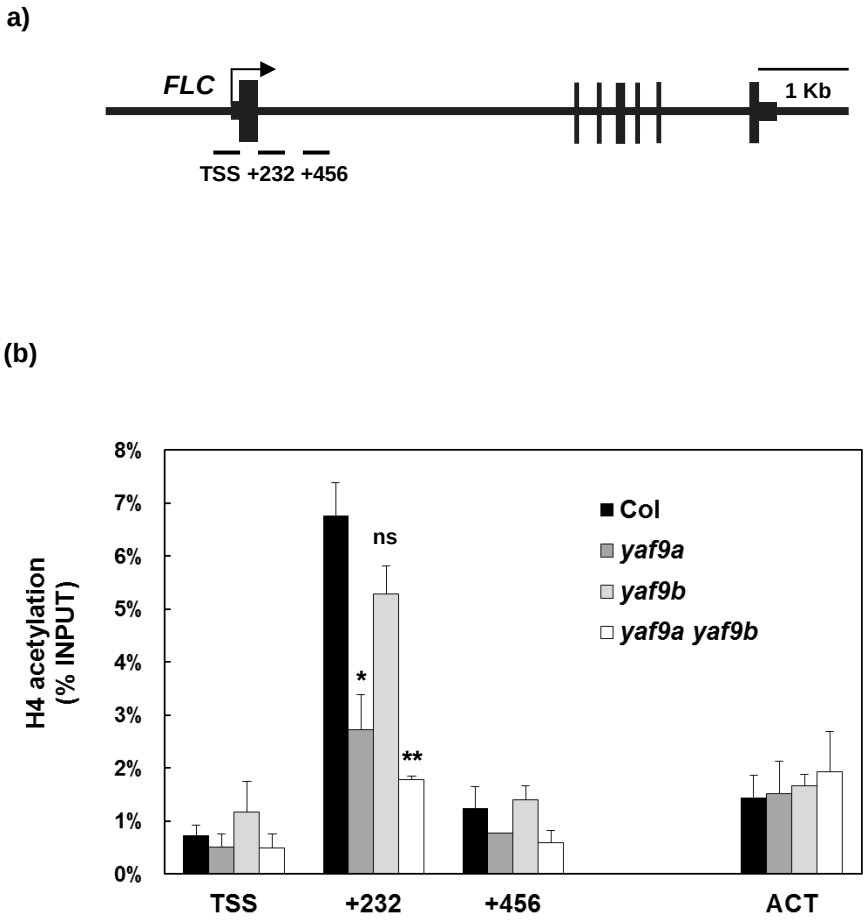

Fig. S14 YAF9A protein directly binds *FT* chromatin and mediates in the deposition of H2A.Z in this locus. (a) Schematic representation of *FT* locus indicating the regions analyzed by ChIP. (b-c) ChIP experiments using α-HTA9 (b) and α-H2AZ.ac (c) in Col, *yaf9 yaf9b* and *arp6* mutant seedlings. Data are represented as the fraction of immunoprecipitated DNA normalized to an *ACT2* gene region. Graphs represent the average of 3 independent biological ChIP experiments quantified by Q-PCR. Error bars indicate ± s.e.m. The statistical significance of the observed difference at region +185 of *FT* chromatin was calculated using Student´s t-test (n.s. not significant, *p≤0.05; **p≤0.01). (d) YAF9-TAPa ChIP experiment using α-Myc. Data are represented as the fraction of immunoprecipitated DNA *FT*/*ACT2* normalized to the values in a control Col line.

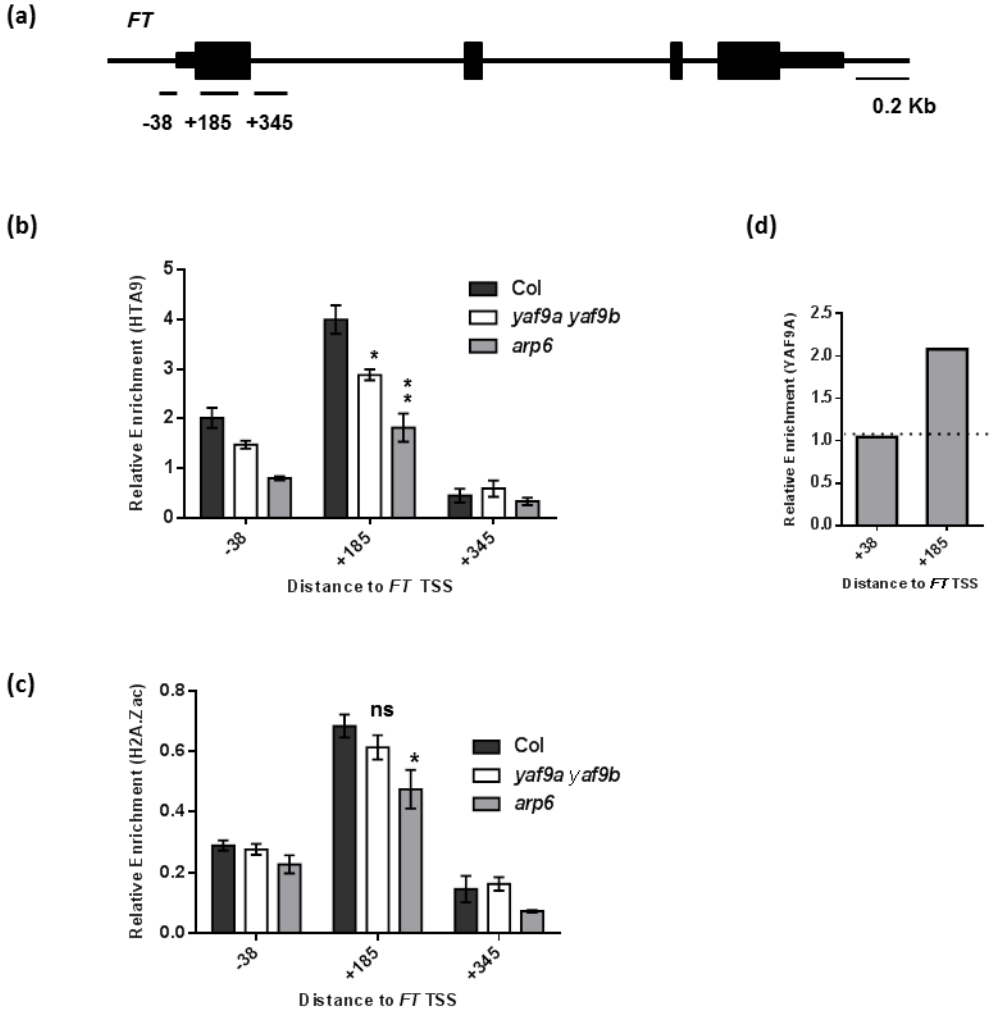

Fig. S15 Characterization of the Arabidopsis *YAF9A-TAPα* 3 and 10 lines generated. (a) Flowering time of *YAF9A-TAPα* lines grown under LD (n=10). Statistical significance was calculated using one-way ANOVA (Tukey test correction for multiple comparisons). Different letters denote a significance level of $p<0.05$; similar letters indicate no significant differences. (b) Q-PCR analysis of the expression of *FLC* in 10 day-old seedlings grown under LD conditions. Error bars indicate ± s.e.m. (n=4). Statistical significance was calculated using one-way ANOVA (Tukey test correction for multiple comparisons). Different letters denote a significance level of $p<0.05$; similar letters indicate no significant differences. (c) Q-PCR analysis of the expression of *YAF9A* in 10 day-old seedlings grown under LD conditions. Error bars indicate ± standard deviation (n=2).

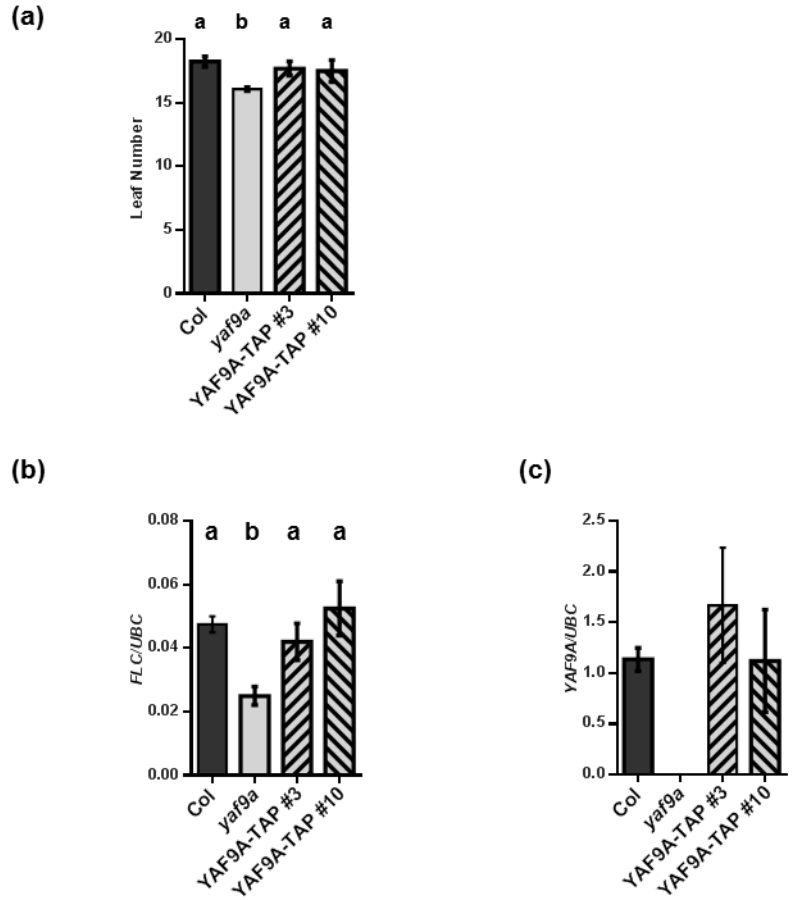

References

Berriri S, Gangappa SN, Kumar SV. 2016. SWR1 chromatin-remodeling complex subunits and H2A.Z have non-overlapping functions in immunity and gene regulation in *Arabidopsis*. *Molecular Plant* **9**: 1051-1065.

Coleman-Derr D, Zilberman D. 2012. Deposition of histone variant H2A.Z within gene bodies regulates responsive genes. *PLOS Genetics:* **8**: e1002988.

Gomez-Zambrano A, Crevillen P, Franco-Zorrilla JM, Lopez JA, Moreno-Romero J, Roszak P, Santos-Gonzalez J, Jurado S, Vazquez J, Kohler C, et al. 2018. *Arabidopsis* SWC4 binds DNA and recruits the SWR1 complex to modulate histone H2A.Z deposition at key regulatory genes. *Molecular Plant* **11**: 815-832.

Kumar SV, Wigge PA. 2010. H2A.Z-containing nucleosomes mediate the thermosensory response in *Arabidopsis*. *Cell* **140**: 136-147.

March-Diaz R, Garcia-Dominguez M, Lozano-Juste J, Leon J, Florencio FJ, Reyes JC. 2008. Histone H2A.Z and homologues of components of the SWR1 complex are required to control immunity in *Arabidopsis*. *Plant Journal* **53**: 475-487.

Zhang H, Richardson DO, Roberts DN, Utley R, Erdjument-Bromage H, Tempst P, Cote J, Cairns BR. 2004. The Yaf9 component of the SWR1 and NuA4 complexes is required for proper gene expression, histone H4 acetylation, and Htz1 replacement near telomeres. *Molecular & Cellular Biology* **24**: 9424-9436

Table S1 . List of oligonucleotides used in this work

GENE	FORWARD	REVERSE	Used for
YAF9A	ACTGGAACAGAGGAGAGAGCC	ATCAATCTCACAAGTGGGCAG	Genotyping *yaf9a-1*
YAF9B	GCCTCCATCGGCTATACAAAG	TGGAGTTGTGAGTTTCCCTTG	Genotyping *yaf9b-2*
YAF9A	ATGACGAACAGCTCGTCATCGAAG	GAGCAGGCAAGTTGTAACCAGAGG	Quantitative RT-PCR
YAF9B	ATGGAGTCGGATATCGAGATTTTGT	GTAGCTCCACGTACATAAACAGTCC	Quantitative RT-PCR
UBQ10	GATCTTTGCCGGAAAACAATTGGAGGATGGT	CGACTTGTCATTAGAAAGAAAGAGATAACACG	Quantitative RT-PCR
FLC	ACTCGGAGTGGGTGAAACTG	CAAAACTTCTTGGCACAGCTC	ChIP region -1155
FLC	ACTATGTAGGCACGACTTTGGTAAC	TGCAGAAAGAACCTCCACTCTAC	ChIP region -335
FLC	GCCCGACGAAGAAAAAGTAG	TCCTCAGGTTTGGGTTCAAG	ChIP region TSS
FLC	CGACAAGTCACCTTCTCCAAA	AGGGGGAACAAATGAAAACC	ChIP region +232
FLC	GGCGGATCTCTTGTTGTTTC	CTTCTTCACGACATTGTTCTTCC	ChIP region +456
FLC	TCATTGGATCTCTCGGATTTG	AGGTCCACAGCAAAGATAGGAA	ChIP region +854
FLC	CTTTTTCATGGGCAGGATCA	TGACATTTGATCCCACAAGC	ChIP region +4260
FLC	CGTGTGAGAATTGCATCGAG	AAAAACGCGCAGAGAGAGAG	ChIP region +6113
FLC	TTGTAAAGTCCGATGGAGACG	ACTCGGCGAGAAAGTTTGTG	ChIP region +6909
FT	TGATTTCACCGACCCGAGTT	AGGCATGAACCCTCTACACATATTTA	ChIP *FT* region -38
FT	GAGACCCTCTTATAGTAAGCAGAGTT	CCTGAGGTCTTCTCCACCA	ChIP region +185
FT	GTTCTTTCACTTGAACTCCCTTTTG	CCCAAGAAATATTTTCAGTATACCCC	ChIP region *+345*
ACT2	TGTCGCCATCCAAGCTGTTCTCT	GTGAGACACCATCACCAGAAT	ChIP *ACTIN 2*
FLC	CCGAACTCATGTTGAAGCTTGTTGAG	CGGAGATTTGTCCAGCAGGTG	Q-PCR expression
FLC	CTGCGACTCAGGGAATCTTCTAA	TTGTGCCATTGAATTGAACCC	Q-PCR expression
YAF9A	ATGACGAACAGCTCGTCATCGAAG	GAGCAGGCAAGTTGTAACCAGAGG	Q-PCR expression
YAF9B	ATGGAGTCGGATATCGAGATTTTGT	GTAGCTCCACGTACATAAACAGTCC	Q-PCR expression
YAF9A	ATGACGAACAGCTCGTCATCGAAG	GAGCAGGCAAGTTGTAACCAGAGG	Q-PCR expression
YAF9B	ATGGAGTCGGATATCGAGATTTTGT	GTAGCTCCACGTACATAAACAGTCC	Q-PCR expression
DREB26	GTGTCCGAAAGAGGAACTGG	TATAGCGGAGGCTCCTTTGA	Q-PCR expression
HAT4	CATGAGCCCACCCACTACTT	ACCTAGGACGAAGAGCGTCA	Q-PCR expression
HB4	ACTCTCACCATGTGCCCTTC	TAGCGACCTGATTTTTGCTG	Q-PCR expression
PI	GAACGCAAACAACAGAGTGG	TGGTCCAACATAGCACCAAG	Q-PCR expression
SEP3	GAGTTTTGCAGTAGTTCGAGCA	GGGTTCTCTGTAAGGCGTCA	Q-PCR expression
JAZ7	AAATGCGACTTGGAACTTCG	CCGAACCGTCTGAACTTCTC	Q-PCR expression
FUL	CCGAGACGTTTCACAAAGTG	TGCTCTTGATAGCTGCATCG	Q-PCR expression
PAR1	TCTCTGTCACCGTCATGCTC	CGCCTCAATCTTTTCCTTGA	Q-PCR expression
PDR12	ATTTGCGATGCTCGTCTTCT	GTTTTCGACAGCTCGACTCC	Q-PCR expression
THI2.1	TCTGGTCATGGCACAAGTTC	GAGTGTTCATGGCACCACAC	Q-PCR expression
PAP1	CGACTGCAACCATCTCAATG	TGTCCCCCTTTTCTGTTGTC	Q-PCR expression
ATACA2	CTTTTCTCGGATTGCTGGAA	CCTTTTTAACGACGGTCCAA	Q-PCR expression

Table S2. List of cell cycle-related genes misregulated in yaf9yaf9b seedlings.

Name	Gene ID	Function	Fold change	p-value
CDC6A	At2g29680	Initiation of replication	+2.69	0.00005455
ORC4	At2g01120	Initiation of replication	+2.18	0.00017657
AUR3	At2g45490	S Phase	+1.77	0.00022055
SMC6B	At5g61460	G2 Phase	+1.68	0.00067999
SMC6A	At5g07660	G2 Phase	+1.43	0.00454551
SKP2A	At1g21410	Mitosis	-1.59	0.00007970

Table S3. List of SAR-related genes deregulated in *yaf9yaf9b* seedlings

Name	Gene ID	Function	Fold change	p-value
ACD6	At4g14400	NPR1 dependent	+4.08	0.00022049
WRKY18	At4g31800	NPR1 dependent	+3.33	0.00208233
ATCNGC11/3	At2g46440	NPR1 dependent	+2.10	0.00509431
NIMIN1	At1g02450	NPR1 dependent	+1.85	0.00005125
PAD4	At3g52430	Upstream from salicylic acid	+1.85	0.00122290
WRKY38	At5g22570	NPR1 dependent	+1.49	0.01391000

Datasets:

Dataset S1. Genome wide transcriptomic analysis of *yaf9a yaf9b* mutants through Affymetrix Microarray (Arabidopsis ATH1 Genome Array) hybridization. File list showing differentially expressed genes ($p<0.05$, $\log_2$fold-change$>\pm0.5$) in *yaf9a yaf9b* compared to WT. Samples collected form 20 day-old seedlings grown on agar plates under SD at ZT8.

Dataset S2. Arabidopsis YAF9A interactors. Proteins co-purified with YAF9A-TAPa in three independent pulldown experiments but not enriched in the control experiment are listed. SWR1-C and NuA4-C related proteins are highlighted in yellow.

Methods S1

Phenotypic analyses and growth conditions

Flowering time was quantified by counting the total leaf number at the time of first flower opening (Lazaro et al., 2008) under both LD and short day (SD) photoperiods. LD conditions consisted of 16 h of light followed by 8 h of darkness, whereas SD conditions corresponded to 8 h of light followed by 16 h of darkness.

Root length was measured in 15 day-old plants grown on vertical plates containing MS medium supplemented with 1% (w/v) sucrose and 1% (w/v) plant agar, at 22°C under LD.

The length of rosette leaves third and fourth, flowers and siliques were measured after fully developed, from at least 15 different plants grown in plastic pots containing a 3:1 mixture of soil and vermiculite substrate in controlled environmental growth chambers at 22°C under LD.

The leaf area quantification data were obtained from the third and fourth rosette leaves of the different genotypes grown on soil under SD conditions during 32 days.

The rosette size was measured as the mean length of the longest leaf (measured as from the centre of the rosette to the furthest edge of the leaf) and the second longest leaf of 4 week-old plants grown under LD. For all size measurements, samples were obtained in a Leica 2000 DM microscope and processed with the ImageJ software 1.34s (Wayne Rasband, National Institutes of Health, USA). Flow cytometry experiments were performed as previously described (Gomez-Zambrano et al., 2018).

Microscopic analyses

Scanning Electron Microscopy (SEM) analyses were performed with plants grown during 32 day-old under SD in soil. These plants were frozen in liquid N2, colored with a colloidal Au/Pd mixture and introduced into the low temperature sample observation (LTSEM) equipment, combined with a Zeiss 960 scanning electron Microscopy. The cells from three different fields and three plants were counted independent, belonging to the 3rd and 4th leaf of the rosette of each of the plants selected. For the analysis of the images obtained, we used the ImageJ 1.34s (Wayne Rasband, National Institutes of Health, USA), which allows quantifying the cell surface of the entire field of vision of three different areas of each leaf.

SDS-PAGE, Western Blotting and histone preparations

Proteins analysis was performed by standards procedures, SDS-PAGE 10% and wet transfer in all the experiments. The polyvinylidene difluoride membrane was blocked with PBS + BSA 3%. Western blot signal was developed using Immobilon Western Chemiluminescent HRP Substrate (Millipore, USA). To detect acetylated histones, seedlings were grown in GM agar plates for 10 days and then incubated for 4 hours in PBS buffer solution supplemented with NaBu 5mM. Histone preparations were performed as described (Gomez-Zambrano *et al.*, 2018).

Co-IP experiments

14 day-old *N. benthamiana* plants were agroinfiltrated with HAM1-HA and YAF9A-GFP gene constructs together with *pCB301-P19* (Voinnet *et al.*, 2003). Samples were harvested at 3 days post-infiltration. The extraction buffer used contained Tris-HCl pH 8, 20 mM, Triton 1%, NaCl

150 mM, EDTA 2.5 mM and cOmplete Protease Inhibitor Cocktail (Roche, Switzerland). Protein extracts were incubated with GFP-Trap-A (Chromotek, Germany) for 1.5 h at 4ºC to allow the immunoprecipitation of YAF9A-GFP and α-HA High Affinity (11867423001 Roche) was used to detect HAM1-HA by Western blot.

Pulldown assays with histone peptides and Arabidopsis histone extracts

YAF9A-GST, YAF9B-GST and GST (in pGEX2TK plasmid) proteins were purified following standard procedures. For the histone peptide pull-down experiments, 1 μg of biotinylated peptide corresponding to the amino acids 1-43 of unmodified histone H3 (Epicypher 12-0065, USA), H3K9ac (Epicypher 12-0003, USA) or H3K27ac (Epicypher 12-0042, USA) were incubated with 5 μl of magnetic Dynabeads M-280 Streptavidin (ThermoFisher Scientific 11205D, USA) for 30 min at 4°C in binding buffer (50 mM Tris pH 7.5, 300 mM NaCl, 0.1% Triton X-100). Peptide-loaded magnetic beads were incubated for 4 h at 4°C with 5 μg of recombinant YAF9A-GST or GST proteins in binding buffer plus protease inhibitors. Then beads were washed four times under stringent conditions (50 mM Tris pH 7.5, 300 mM NaCl, 1% Triton X-100, 0.1% SDS). Pull-down proteins were detected by western blot using α-GST (GE Healthcare 27-4577, USA).

For histone extracts pull-down assays, we first purified Arabidopsis histones extracts from MM2d cell suspensions following established protocols (Lopez-Gonzalez *et al.*, 2014). Later on, 2 μg of recombinant YAF9A-GST, YAF9B-GST or GST proteins bound to glutathione sepharose beads (Amersham, UK) were incubated with 10 μg of histone extracts for 2 h at 4°C in binding buffer (50 mM Tris pH 7.5, 150 mM NaCl, 0.1% Triton X-100). Then, beads were washed with PBS-T buffer several times and histones were detected by western blot using α-H3 (Abcam ab1791, UK), α-H3ac (K9ac/K14ac; Millipore 06-599, USA) and α-H2B (Active Motif 39947, USA).

Protein affinity purification and tandem mass spectrometry

Functional *2x35S::YAF9A::TAPa* overexpressing transgenic line 3 was used for protein affinity purification (Fig. S13). Tandem affinity purification was performed as described (Rubio *et al.*, 2005) with slight modifications. Protein extraction was performed using the same buffer (Tris-HCl pH7.5 10 mM, NaCl 150 mM, EDTA 2.5 mM, DTT 1 mM, Glycerol 10% and Triton X-100 0.5%, supplemented with cOmplete Protease Inhibitor Cocktail (Roche, Switzerland)) from 10 g of seedlings material. First immunoprecipitation was performed using Sepharose IgG beads (Amersham), and purified YAF9A proteins were released using 3C protease (Amersham, UK); second purification step was performed using HisPur Ni-NTA Resin (ThermoFisher Scientific, USA) and proteins were eluted using Imidazole 200 mM. All procedures were carried out at 4°C. We performed three *YAF9A::TAPa* pull-down biological replicates and the corresponding control protein purification from WT. Proteomics data analysis was performed as described (Gomez-Zambrano *et al.*, 2018) and the identified peptides are listed in Dataset S2.

References

Gomez-Zambrano A, Crevillen P, Franco-Zorrilla JM, Lopez JA, Moreno-Romero J, Roszak P, Santos-Gonzalez J, Jurado S, Vazquez J, Kohler C, et al. 2018. *Arabidopsis* SWC4 binds DNA and recruits the SWR1 complex to modulate histone H2A.Z deposition at key regulatory genes. *Molecular Plant* **11**, 815-832

Lazaro A, Gomez-Zambrano A, Lopez-Gonzalez L, Pineiro M, Jarillo JA. 2008. Mutations in the Arabidopsis *SWC6* gene, encoding a component of the SWR1 chromatin remodelling complex, accelerate flowering time and alter leaf and flower development. *Journal of Experimental Botany* **59**: 653-666.

Lopez-Gonzalez L, Mouriz A, Narro-Diego L, Bustos R, Martinez-Zapater JM, Jarillo JA, Pineiro M. 2014. Chromatin-dependent repression of the Arabidopsis floral integrator genes involves plant specific PHD-containing proteins. *Plant Cell* **26**: 3922-3938.

Rubio V, Shen Y, Saijo Y, Liu Y, Gusmaroli G, Dinesh-Kumar SP, Deng XW. 2005. An alternative tandem affinity purification strategy applied to Arabidopsis protein complex isolation. *Plant Journal* **41**: 767-778.

Voinnet O, Rivas S, Mestre P, Baulcombe D. **2003**. An enhanced transient expression system in plants based on suppression of gene silencing by the p19 protein of tomato bushy stunt virus. *Plant Journal* **33**: 949-956.